

Homogenization and effective properties formulations for propagation in finely structured laminates — a multi-resolution approach

Ben Zion Steinberg

Department of Interdisciplinary Studies, Faculty of Engineering, Tel-Aviv University, Tel-Aviv 69978, Israel

Received 4 December 2000; accepted 5 March 2001

Abstract

Multi-resolution approach is used to derive homogenized (large scale) formulation for propagation of waves in complex laminates. Basic entities such as boundary conditions, spatial and temporal spectrum (eigenvalues and resonances), Wronskian, modal expansions, and Green function representations associated with the homogenized formulation are discussed. The relations between them and their generic (all-scales, or *complete*) counterparts are studied. The dependence of these relations on parameters such as excitation frequency and heterogeneity length-scale are explored. © 2001 Elsevier Science B.V. All rights reserved.

1. Introduction

The propagation of time-harmonic field of frequency ω in a homogeneous medium, remote from the source region, can be characterized by a single length-scale — the wavelength λ . We shall use λ as a discriminator of the range of length-scales pertaining to any propagation/scattering scenario embedded in that medium. Thus, length-scales on the order of λ and above are termed *macro-scales* and length-scales much smaller than λ (say $\lambda/10$ and below) are termed as *micro-scales*.

We are concerned with *complex heterogeneity*, defined as micro-scale variation of the medium properties (say ϵ or μ or both), occupying space domains of macro-scale size, with the possible presence of macro-scale variation. An example is shown in Fig. 1. When a wave interacts with such a medium, the field within and near the complex heterogeneity may “inherit” the medium complexity — it contains a wide range of length-scales, from micro to macro. The development of *complete* propagation/scattering formulations capable of coping with the articulated complexity introduces significant challenges (“complete” means the incorporation of all length-scales). Traditional high-frequency asymptotics cease to be valid when the heterogeneity length-scale becomes small relative to λ , and traditional numerical procedures may become too large to handle.

However, in many problems of interest, the field *observables* — e.g. far field radiation pattern, field measured by a detector with finite spatial resolution, and so on — are determined only by the *macro-scale component of the response*, while the micro-scale component is practically irrelevant. This observation suggests a potential remedy — the development of new propagation/scattering formulations tuned to govern only the macro-scale component of the field, say $u^s(r)$.

E-mail address: steinber@eng.tau.ac.il (B.Z. Steinberg).

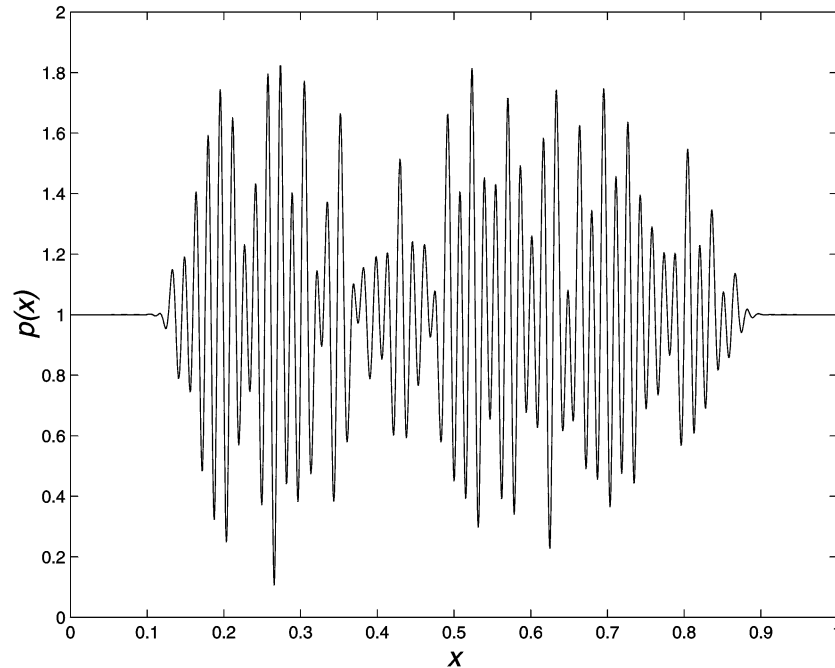


Fig. 1. An example of complex heterogeneity.

The role of homogenization is to develop self-consistent *effective* or *homogenized* formulations governing u^s only. In these formulations the complex heterogeneities $\epsilon(r)$, $\mu(r)$ are replaced by their effective measures $\epsilon^e(r)$, $\mu^e(r)$ — simpler (smoother) functions or *operators* that comprise macro-scale only and can faithfully represent the footprint of the micro-scale heterogeneity on the macro-scale field. Once the effective measures are obtained, a plethora of analytical, asymptotic, and numerical techniques is available to solve the homogenized problem. For example, one may hope to develop “effective modal analysis” and “effective ray/WKB theory” based on the effective measures.

Thus, our goal is not only to “homogenize” the relevant PDEs, but also to develop a practical *effective wave theory*. We purposefully emphasize “theory” — a framework that can address the following “vertical” issues (how can we use homogenization efficiently?) and “horizontal” issues (how its basic entities relate to those of the complete formulation?), as schematized in Fig. 2:

1. *Rules for anticipating the existence of a footprint.* Is it possible to devise rules that predict a priori which types of micro-scale heterogeneities carry a footprint on the macro-scale response, and which practically do not? The effective measures of the latter are their macro-scale components, while those of the former are more difficult to obtain.
2. *Boundary conditions (BC) for the homogenized formulation.* The generic BC, obtained from basic physical laws, apply to the *complete* field. What are the appropriate BC for the macro-scale field? In particular, in what cases the generic BC apply to the homogenized formulation as well?
3. *Spectral equivalence.* How the spectrum of the homogenized formulation relates to that of the complete one? Denote the modes and eigenvalues of the former and the latter by (u_n^*, λ_n^*) and (u_n, λ_n) , respectively. Then, under what conditions (e.g. mode order n , micro-structure length-scale ℓ , frequency, etc.) u_n^* gives the macro-scale component of u_n (u_n^s) and $\lambda_n^* = \lambda_n$ (spectral equivalence), at least in some asymptotic sense? The same question is raised about the resonance frequencies Ω_n^* and Ω_n . The spectral equivalence is essential for equating the field expansion in the homogenized formulation to that in the complete one, and for assigning *the same physical interpretation to corresponding building blocks*.

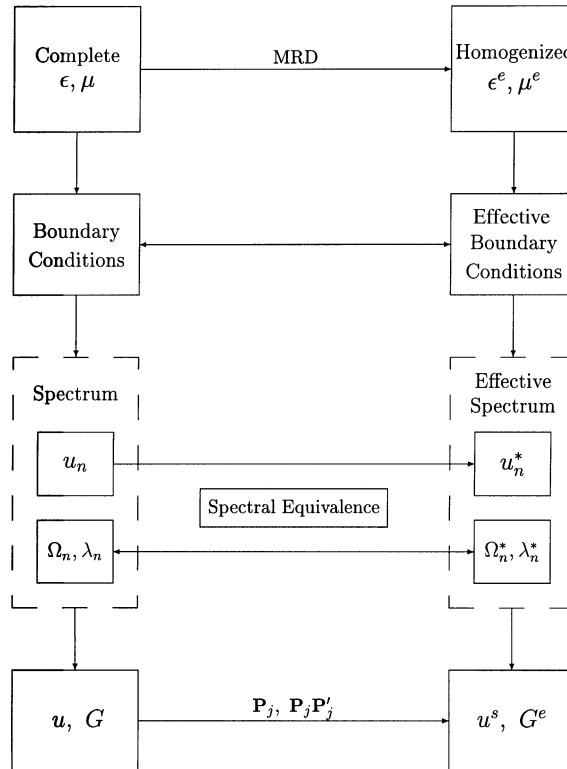


Fig. 2. The building blocks of effective wave theory and the associated inter-relations.

4. *The fundamental source problem.* Since homogenization is about large scale solutions, self-consistency requires the homogenized formulation Green function to contain no micro-scale components, at least formally. Thus one must establish a relation between the Green function of the complete formulation and that of the effective one in terms of relations between the fundamental sources or in terms of relations between the corresponding spectral representations.

Traditional homogenization techniques were developed for periodic structures. They are based on establishing a weak asymptotic limit as the length-scale of the micro-structure becomes infinitely small compare to the macro-scale [1]. The across-scales coupling phenomenology is not expressed explicitly as part of the mathematical procedure, and the physical/mathematical mechanisms underlying it remain obscured. Most of the issues articulated above are not treated.

The formulation developed in [2–9] is based on a different approach and is formally free from these limitations. Multi-resolution analysis (MRA) [10] and wavelet transforms are applied to the integral operator representation of the propagation/scattering scenario. This decomposes the latter into a hierarchy of scales, ranging from micro to macro, and forms a convenient starting point for a study of the across-scales phenomenology and for a new homogenization scheme, free from the classical limitations. A self-consistent formulation governing the macro-scale response can then be derived by applying Schur’s complement procedure. The result is an effective (homogenized) formulation, where the footprint of the micro-scale heterogeneity on the macro-scale response is expressed via an *effective material operator* (EMO).

The main features of the EMO were studied in [2–7] for electromagnetic and acoustic scattering in several simple canonical configurations. Refs. [4,6] reconstruct the classical result of homogenization of the equation $(Qu')' = f$, but free from the classical limitations. A study of the MRA homogenization within the framework of Sturm–Liouville

equations on a closed domain has been carried out in [8,9]. It has been shown that for Neumann, Dirichlet, and certain types of impedance BC, the generic BC applies to the homogenized formulation as well. This work has also explored the relationship between the eigenvalues and eigenfunctions of the complete and of the homogenized (effective) Sturm–Liouville problems, and in particular has established the conditions for spectral equivalence. These fundamental spectral results have been later applied in [11,12] to formulate effective modal propagation schemes in complex layered ducts and an “effective vertical-modes/horizontal-rays” scheme for slowly varying complex stratifications.

We note that MRA and wavelets have been used recently by Brewster and Beylkin [13] for numerical homogenization. The basic ideas are similar to those developed in [2,3]. The work in [13] is devoted mainly to a sophisticated “decimation” process in which an efficient numerical algorithm for estimating the large scale response component is developed. It does not address directly the questions articulated above. Using the multi-resolution approach, the classical result was re-derived later by Gilbert [14], together with a correction term. In [15], the algorithm developed in [13] is used to investigate the numerical homogenization of boundary value problems. Their work, however, does not provide analytic expression for the effective properties, and does not address the issue of the appropriate boundary conditions for the homogenized problem.

The purpose of the present work is to use the multi-resolution homogenization scheme to derive a systematic effective modal analysis for electro-magnetic propagation in complex ducts. This will be based on the extension of the results reported in [8,9] to the relevant propagation problems. Thus, effective properties, BC, and spectral equivalence will be examined for a Sturm–Liouville equation that is more general than that treated in [8,9] and better suited to electromagnetic wave propagation. For convenience we start with a summary of the main results derived before. Based on this, three new inequalities (2.13), (2.17) and (2.18), are obtained. These inequalities are used here for: (a) Extending the spectral equivalence theorem of Steinberg et al. [8] for cases including *two* heterogeneity functions (this was discussed in [9], but not derived or proved). (b) Demonstrating a *new* relation between the *Wronskians* of the generic and homogenized formulations. This result is important for generalizing the spectral equivalence theorem also for resonance frequencies. (c) Developing modal expansion schemes for the Green functions and for source-free propagation fields.

2. The multi-resolution approach to homogenization

2.1. Wavelets, scaling functions, and smoothing

Let $\{V_j\}_{j \in \mathbb{Z}}$ be a nested sequence of linear spaces that constitutes a multi-resolution decomposition (MRD) of $L_2(R)$ (\mathbb{Z} is the set of all integers). Let $\phi(x)$ and $\psi(x)$ be the corresponding scaling function and wavelet, respectively. The function $\phi_{jn}(x)$ is defined via $\phi(x)$ as $\phi_{jn}(x) = 2^{j/2} \phi(2^j x - n)$, and a similar definition holds for $\psi_{mn}(x)$. Then, $\{\phi_{jn}\}_{n \in \mathbb{Z}}$ is an orthogonal basis of V_j , and $\{\psi_{jn}\}_{n \in \mathbb{Z}}$ is an orthogonal basis of O_j , the orthogonal complement of V_j in V_{j+1} . The spectrum of $\phi_{jn}(x)$ is centered in the low frequency regime $|\xi| \leq 2^j$, while that of $\psi_{jn}(x)$ is centered in the band-pass regime $2^j \leq |\xi| \leq 2^{j+1}$. Examples are shown in Fig. 3. An approximation of a field $u(x)$ at a resolution k can be written as the sum of two mutually orthogonal fields, namely a smooth (u^s , macro-scale) and a detail (u^d , micro-scale) components. We have $u(x) = u^s(x) + u^d(x)$, where

$$u^s(x) = \mathbf{P}_j u(x) = \sum_n s_n \phi_{jn}(x), \quad s_n = \langle u, \phi_{jn} \rangle, \quad (2.1a)$$

$$u^d(x) = \mathbf{D}_j^k u(x) = \sum_{m=j}^{k-1} \sum_n d_{mn} \psi_{mn}(x), \quad d_{mn} = \langle u, \psi_{mn} \rangle. \quad (2.1b)$$

Here, $\langle \cdot, \cdot \rangle$ denotes the inner product of $L_2(R)$, and $j < k$ is the reference smoothing resolution. $u^s(x)$ can be interpreted as the spatial average of $u(x)$, with the averages being taken over intervals of the size 2^{-j} . The

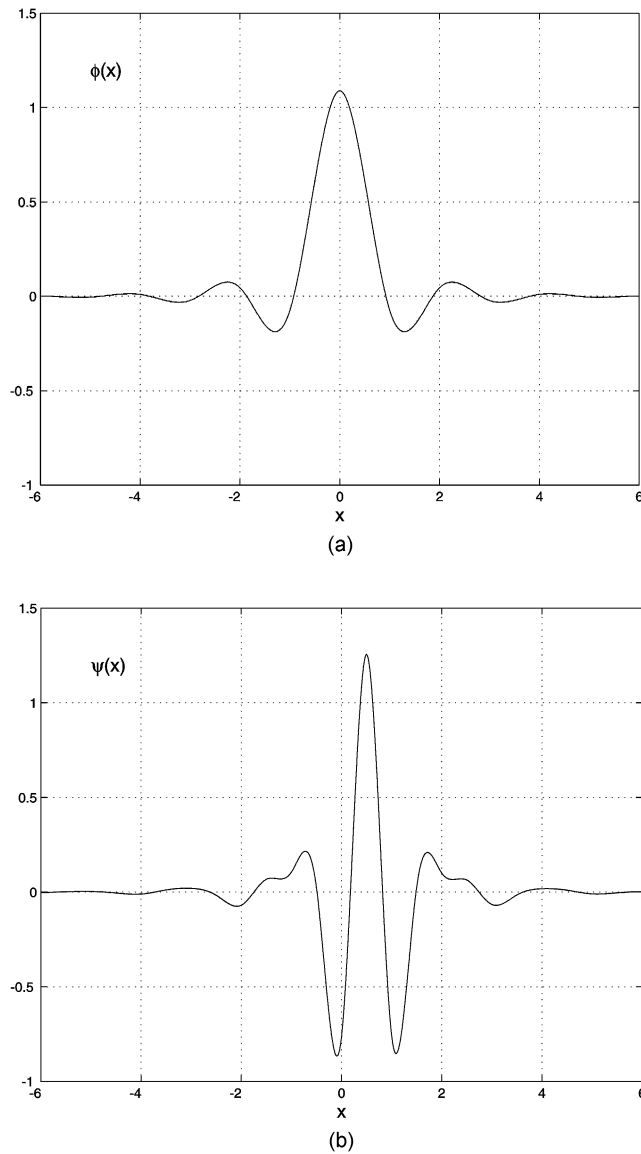


Fig. 3. The cubic spline Battle–Lemarie: (a) scaling function ϕ , (b) wavelet ψ .

field component $u^d(x)$ contains the remaining fine details. The resolution level j should be chosen such that u^s faithfully describes field components possessing spatial length-scales in the order of a wavelength λ and larger. For a normalized wavelength $\lambda = 1$, we choose $j = 3$.

2.2. Construction of the homogenized formulation—the basic apparatus

One may address the difficulty of boundary conditions (see issue (2) in Section 1) by rewriting the boundary value problem in terms of a second kind Fredholm integral equation (known also as a Lippman–Schwinger equation). In the latter *the boundary conditions are incorporated in the structure of the integral kernel*, and are not specified

explicitly “at a point”. Thus, the incorporation of new “effective” boundary conditions in homogenized formulation comes out naturally as a mapping of the integral kernel function. As shown in [8] this indeed is the case, although some exceptions may occur. Thus, we first cast the propagation/scattering problem in integral equation form and then apply the homogenization procedure.

A general form of the integral equation is given by

$$u(x) = u_0(x) + \mathbf{L}u, \quad (2.2a)$$

where u is the response field to be determined, \mathbf{L} is a linear operator

$$\mathbf{L}u = \int_a^b k(x, y)q(y)u(y) dy = \mathbf{L}_b(qu), \quad (2.2b)$$

$q(x)$ is the heterogeneity function, and $k(x, y)$ is a known kernel, related (but not always identical) to the Green function of a properly defined homogeneous background problem. $u_0(x)$ is a known forcing term interpreted as the system response in the absence of the heterogeneity ($q = 0$). Projecting this operator equation onto the nested sequence of linear spaces $\{V_j\}_{j \in \mathbb{Z}}$, via a Galerkin procedure with Eqs. (2.1a) and (2.1b), we get the set of equations

$$\begin{pmatrix} \mathbf{I} - \Phi & -\mathbf{C} \\ -\bar{\mathbf{C}} & \mathbf{I} - \Psi \end{pmatrix} \begin{pmatrix} \vec{s} \\ \vec{d} \end{pmatrix} = \begin{pmatrix} \vec{s}_0 \\ 0 \end{pmatrix}, \quad (2.3)$$

where the coefficients of the macro-scale field u^s and the micro-scale field u^d are collected in \vec{s} and \vec{d} , respectively. The same interpretation holds for the known scaling functions coefficients vector \vec{s}_0 —it is associated with the forcing $u_0(x)$ large scale component. Since this forcing is nothing but the system response in the absence of the heterogeneity (when $q = 0$), it contains no micro-scale component. Hence, the null vector in the lower part of the r.h.s. in Eq. (2.3). \mathbf{I} is the identity matrix and Φ , \mathbf{C} , $\bar{\mathbf{C}}$ and Ψ are matrix operators with elements $\Phi_{n',n} = \langle \mathbf{L}\phi_{jn}, \phi_{jn'} \rangle$, $C_{n',mn} = \langle \mathbf{L}\psi_{mn}, \phi_{jn'} \rangle$, $\bar{C}_{m'n',n} = \langle \mathbf{L}\phi_{jn}, \psi_{m'n'} \rangle$, $\Psi_{m'n',mn} = \langle \mathbf{L}\psi_{mn}, \psi_{m'n'} \rangle$. The set in Eq. (2.3) provides the starting point for a multi-resolution study of the propagation/scattering problem. From the lower half of Eq. (2.3) the response detail component \vec{d} can be expressed in terms of the response large scale component \vec{s} . When the result is substituted into the upper half of Eq. (2.3), we get a formulation governing \vec{s}

$$[\mathbf{I} - \Phi - \mathbf{C}(\mathbf{I} - \Psi)^{-1}\bar{\mathbf{C}}]\vec{s} = \vec{s}_0. \quad (2.4)$$

This formulation is the basic MRA homogenization scheme. The information of the small scale heterogeneity $q^d(x)$ appears essentially in $\mathbf{C}(\mathbf{I} - \Psi)^{-1}\bar{\mathbf{C}}$. Thus, it is the EMO, which describes how the micro-scale heterogeneity $q^d(x)$ affects the macro-scale response. A general measure of the potential degree of this effect is the EMO norm. If $\|\text{EMO}\| \ll \|\Phi\|$ then the small scale heterogeneity has practically no effect on the large scale response. If these norms are comparable then a small scale heterogeneity can have a significant effect on the large scale response. Thus, an estimate of the EMO norm can provide the rule discussed in (1) in Section 1. The integral kernel $k(x, y)$ is closely related to the background problem Green function $G^b(x, y)$ (see Section 3). The latter is singular at $x = y$. Similarly, one may expect that the heterogeneity function $q(x)$ possesses a non-regular behavior of some order. These properties can be used in conjunction with theorems on wavelets near singularities [10] to obtain estimates on the norm bounds (see [8]). We have the following theorem.

Theorem 2.1. *Let $k(x, y)$ be the integral operator kernel. Let $k(\cdot, y) \in C^p$, $q(\cdot) \in C^{p'}$ with $p, p' \geq 0$, and $\phi(x), \psi(x) \in C^N$ with $N > \max(p, p')$. Then, if $\|q\| = O(1)$:*

$$\|\Psi\|^2 \leq cN_0^2 \frac{2^{-2j(p'+p+2)}}{[1 - 2^{-2(p+1)}][1 - 2^{-2(p'+1)}]}, \quad (2.5a)$$

$$\|\bar{\mathbf{C}}\|^2 \leq cN_0^2 \frac{2^{-2j(p+1)}}{1 - 2^{-2(p+1)}}, \quad (2.5b)$$

$$\|\mathbf{C}\|^2 \leq cN_0^2 \frac{2^{-2j(p'+1)}}{1 - 2^{-2(p'+1)}}, \tag{2.5c}$$

$$|\bar{C}_{m',n}| \leq cN_0 2^{-m'(p+3/2)}, \tag{2.5d}$$

where $c = O(1)$, N_0 is the number of resolution 0 grid points covering the domain of interest.

The EMO norm bound is dominated by the regularity of the integral equation kernel. The latter is closely related to the *near field structure* of the background problem Greens function. This is a formal connection between the waves *physics* and the across-scale coupling phenomenology. But also, it provides a rule for distinguishing between the heterogeneities that carry a footprint and those which do not, see issue (1) in Section 1. The procedure goes as follows. (a) Cast the problem in the form of a Fredholm integral equation. (b) Check the singularity nature of the associated kernel $k(x, y)$ and heterogeneity. For smooth or mildly singular ones, $\|\text{EMO}\| \ll 1$ and the micro-structure practically has no footprint in $u^s(x)$. For strongly singular ones, the EMO norm is significant and the heterogeneity can have a profound footprint. Below, we contrast the two extremes of weakly singular kernel vs. strongly singular (possessing δ singularity) one. They will be found useful in Section 3.

2.2.1. The weakly singular case

Here $\|\bar{\mathbf{C}}\| \ll 1$, $\|\Psi\| \ll 1$. Thus, we have from the lower part of Eq. (2.3)

$$\|u^d(x)\| \ll \|u^s\|. \tag{2.6}$$

Furthermore, here $\|\text{EMO}\| \ll 1$, so Eq. (2.4) can be replaced by

$$[\mathbf{I} - \Phi]\vec{s} = \vec{s}_0. \tag{2.7}$$

The elements of the matrix operator Φ can be written as (\mathbf{L}_b^* is the adjoint of \mathbf{L}_b):

$$\Phi_{n',n} = \langle \mathbf{L}_b q \phi_{jn}, \phi_{jn'} \rangle = \langle q \phi_{jn}, \mathbf{L}_b^* \phi_{jn'} \rangle = \langle q \phi_{jn}, \phi_{jn'}^f \rangle. \tag{2.8}$$

Recall, however, that the kernel $k(x, y)$ is related to the *background* problem, thus away from the origin it comprises macro-scales only. Together with the condition that the irregularity at the origin is weak, we can approximate

$$\phi_{jn}^f(x) \approx 2^{-j/2} \overline{k(y_{jn}, x)}, \quad y_{jn} = n2^{-j}, \tag{2.9}$$

which again, comprises macro-scales only (an overline denotes complex conjugate). Thus, $\Phi_{n',n}$ can be rewritten as

$$\Phi_{n',n} = \langle q^s \phi_{jn}, \phi_{jn'}^f \rangle = \langle \mathbf{L}_b q^s \phi_{jn}, \phi_{jn'} \rangle. \tag{2.10}$$

The last result means that the only relevant measure that affects u^s is q^s . Furthermore, there is a *conservation of structure* here: the kernel associated with $\Phi_{n',n}$ above is the same as that associated with the original integral equation. Using this result in Eq. (2.7) and reversing the steps back to an integral equation, we get

$$u^s(x) = u_0(x) + \mathbf{L}_b q^s u^s \tag{2.11}$$

that means the effective measure is simply q^s (compare with Eqs. (2.2a) and (2.2b)). Furthermore, since the kernel here is the same as the one associated with the complete problem (2.2a), the generic BC apply to the effective formulation as well.

From the structure of the matrix equation (2.3) it can be shown that if q^d possesses scales not larger than a given micro-scale 2^{-m_i} , so does u^d . Then, a more precise estimate on the relation between u^d and u^s can be derived. From

Eq. (2.3), we have $\vec{d} \approx \bar{\mathbf{C}}\vec{s}$. Thus, the mn wavelet coefficient in \vec{d} is given by $(\vec{d})_{mn} = \sum_{n'} \bar{C}_{mn,n'}(\vec{s})_{n'}$. Together with the bound in Eq. (2.5d) it gives

$$|(\vec{d})_{mn}| \leq \sum_{n'} |\bar{C}_{mn,n'}| |(\vec{s})_{n'}| \leq cN_0 \max_{n'} |(\vec{s})_{n'}| 2^{-m(p+3/2)}, \quad (2.12)$$

where N_0 and p are defined in Theorem 2.1, and $c = O(1)$. With the Parseval identity, we find

$$\begin{aligned} \|u^d\|^2 &= \sum_{m=m_i}^{\infty} \sum_n |(\vec{d})_{mn}|^2 \\ &\leq c \|u^s\|^2 \sum_{m=m_i}^{\infty} \sum_n 2^{-2m(p+3/2)} \quad \text{with Eq. (2.12)} \\ &\leq c \|u^s\|^2 N_0 \sum_{m=m_i}^{\infty} 2^{-2m(p+1)} \quad \text{there are } N_0 2^m \text{ points in resolution } m \\ &= \frac{c \|u^s\|^2 N_0 2^{-2m_i(p+1)}}{1 - 2^{-2(p+1)}}. \end{aligned} \quad (2.13)$$

Thus, as the micro-scale becomes smaller, so does $\|u^d\|/\|u^s\|$.

2.2.2. The strongly singular case

Here, we assume that $k(x, y)$ can be written as

$$k(x, y) = \Gamma(x, y) - \delta(x - y), \quad (2.14)$$

where $\delta(x)$ is the Dirac δ , and $\Gamma(x, y)$ has the same properties as $k(x, y)$ of Section 2.2.1. With the strongly singular term in $k(x, y)$, the EMO cannot be neglected, so $q^d(x)$ can have a profound footprint in the macro-scale response. Due to the simplicity of $k(x, y)$, one can obtain simple expressions for the effective measures. By substituting Eq. (2.14) into Eq. (2.2a) and performing the integration over the δ term, we obtain a new integral equation:

$$T(x) = u_0(x) + \Gamma_b \left(\frac{q}{Q} T \right), \quad (2.15a)$$

where Q and T are new functions and Γ_b is a new operator

$$Q(x) = 1 + q(x), \quad T(x) = Q(x)u(x), \quad \Gamma_b f = \int_a^b \Gamma(x, y) f(y) dy. \quad (2.15b)$$

Since the kernel of Γ_b is the function Γ , this operator possesses now exactly the same features as \mathbf{L}_b of Section 2.2.1, and the results obtained there for u can be directly applied here for T . Therefore, we have from Eq. (2.6) (or Eq. (2.13)) and Eq. (2.11)

$$\|T^d(x)\| \ll \|T^s\|, \quad T^s(x) = u_0(x) + \Gamma_b \left(\left(\frac{q}{Q} \right)^s T^s \right). \quad (2.15c)$$

However, from Eq. (2.15b), we have $u = Q^{-1}T$, and from the first part of Eq. (2.15c) (or from Eq. (2.13) which applies here for T), we have $u^s = (Q^{-1})^s T^s$. Reversing this last equation to express T^s in terms of u^s and substituting the result back to Eq. (2.15c) yields finally an homogenized integral equation for u^s

$$u^s(x) = u_0(x) + \mathbf{L}_b(q^e u^s), \quad q^e = \left[\left(\frac{1}{Q(x)} \right)^s \right]^{-1} - 1, \quad (2.16)$$

where the integral operator \mathbf{L}_b is the same as the generic one, its kernel is given by Eq. (2.14). Thus, q^e above is the effective measure of q , and the homogenized formulation possesses the same boundary conditions as the complete one.

When the kernel is of the form in (2.14), a correction term representing the δ contribution should be added to the bounds in Eqs. (2.5a)–(2.5d). For $\tilde{C}_{m'n',n}$ the added term is $cN_02^{-m'(p'+3/2)}$ (assuming $\|q\| = O(1)$). Following now the derivations in Eqs. (2.12) and (2.13), we get

$$\|u^d\|^2 \leq \frac{c\|u^s\|^2 N_0 2^{-2m_i(\sigma+1)}}{1 - 2^{-2(\sigma+1)}}, \quad \sigma = \min(p, p'), \tag{2.17}$$

where p, p' apply now to the regularity of Γ, q , respectively. Thus, also in the case of highly singular kernel, $\|u^d\|/\|u^s\|$ decreases as the micro-scale decreases.

From the relation $u = (Q^{-1})T$ and from Eq. (2.15c) (or from Eq. (2.13) which applies here for T), we obtain the following smoothing rule:

$$(Qu)^s = Q^e u^s + \tilde{R}, \quad \|\tilde{R}\| \leq c\|T^s\|2^{-m_i(p+1)}, \tag{2.18}$$

which will be found useful in subsequent derivations.

3. Applications to propagation in complex laminates

3.1. The basic equations

We start with a 1D Sturm–Liouville equation (the complete problem)

$$\left[\frac{d}{dx} Q(x) \frac{d}{dx} + \Omega^2 M(x) \right] u(x) = F(x), \quad a \leq x \leq b \tag{3.1}$$

with Neumann or Dirichlet BC, and with $\Omega = O(1)$. The functions Q and M represent the heterogeneity. When these are identically equal to 1, the length-scale of u is in the order of $\Omega^{-1} = O(1)$ — the macro-scale. For simplicity of derivation, we distinguish between three cases:

1. $Q = 1$, and $M = 1 + m(x)$ possesses a micro-structure. Here, the governing integral equation is of the type discussed in Section 2.2.1 (the derivation is outlined in Appendix A). Thus, for this case $M^e = M^s(x)$, with the same BC as the complete formulation.
2. $M = 1$, and $Q = 1 + q(x)$ possesses a micro-structure. Here, the governing integral equation has the same structure as that in Section 2.2.2. This case was treated in detail in [8], see Appendix A for the derivation outlines. Thus, here we have $Q^e = [(Q^{-1})^s]^{-1}$. The corresponding boundary conditions are summarized in Table 1.
3. $Q = 1 + q(x)$, $M = 1 + m(x)$ both possess micro-structure. Here, one cannot obtain a single integral equation of the structure discussed in Section 2.2. However, we can still obtain effective measures by applying the two-step procedure described preliminary in [11]. Define the Green function G_M :

$$\left[\frac{d^2}{dx^2} + \Omega^2 M(x) \right] G_M(x; y) = -\delta(x - y). \tag{3.2}$$

Using the results of case 1 and Section 2.2.1, it can be shown that $G_M^s = G_{M^s}$, where the smoothing on the l.h.s. operates on both x and y . Furthermore, we have $\|G_M^d\| \ll \|G_M^s\|$, so to a very good approximation $G_M = G_{M^s}$.

Table 1
The complete (all scales) and effective boundary conditions

Boundary conditions	Complete	Effective
Dirichlet	$u = 0$	$u^s = 0$
Neumann	$v = 0$	$v^s = 0$
Natural impedance	$\alpha u + Qv = 0$	$\alpha u^s + Q^e v^s = 0$

Use G_M as a background problem Green function to obtain an integral equation formulation for u with both Q and M present, and invoke the last approximation. The result is

$$u(x) = u_0(x) + \int_a^b G_{M^s}(x, y)(q(y)u'(y))' dy. \quad (3.3)$$

Although, explicit expressions of G_M are not available for general M , some basic properties always hold: it is continuous at $x = y$, and its second mixed derivative results in a δ distribution and a continuous term. Furthermore, since $\|G_M^d\| \ll \|G_M^s\|$, it consists of macro-scale only away from the diagonal. Thus, Eq. (3.3) possesses exactly the same properties as Eq. (A.1). Continue from this point by following exactly the same steps described in Appendix A. The final result is that q^e is the same as in the previous case. Thus the homogenized formulation is

$$\left[\frac{d}{dx} Q^e(x) \frac{d}{dx} + \Omega^2 M^e(x) \right] u^s(x) = F(x), \quad a \leq x \leq b, \quad (3.4a)$$

where the effective properties are given by

$$M^e = M^s(x), \quad Q^e = [(Q^{-1})^s]^{-1}, \quad (3.4b)$$

and with the same BC as that of case 2 (see Table 1). The smoothing relation of Eq. (2.18) still holds, but for the quantity governed by the integral equation. Thus ($v = u'$):

$$(Qv)^s = Q^e v^s + \tilde{R}, \quad \|\tilde{R}\|, \|(Qv)^d\| \leq c\|(Qv)^s\| 2^{-m_i(p+1)}. \quad (3.5)$$

Furthermore, the relation in (2.17) applies here as well.

3.1.1. Spectral properties

We wish to study how the eigenvalues and eigenfunctions of the complete formulation relate to those of the effective one. Two new aspects of the spectral equivalence are discussed here. These are the presence of an additional heterogeneity function $M(x)$, and the role of the frequency parameter Ω . We start with the following simple theorem (see [8] for a proof).

Theorem 3.1. *Let $\{f_n^\ell\}$ be an orthonormal basis in a Hilbert space H that depends on the parameter ℓ . Let $\{g_n\}$ be an orthonormal sequence in H . If $\forall m \neq n \langle f_n^\ell, g_m \rangle \rightarrow 0$ as $\ell \rightarrow 0$, then $f_n^\ell \rightarrow g_n$ as $\ell \rightarrow 0 \forall n$.*

We shall use this theorem to establish a spectral equivalence. Let $u_n(x)$, λ_n be the n th eigenfunction and eigenvalue associated with the complete formulation in Eq. (3.1) with $M(x) = R(x) + \lambda W(x)$. Let $u_n^*(x)$, λ_n^* be those associated with the effective formulation in Eqs. (3.4a) and (3.4b). The pairs u_n, λ_n and u_m^*, λ_m^* satisfy

$$(Qv_n)' + \Omega^2 R u_n + \Omega^2 \lambda_n W u_n = 0, \quad (3.6a)$$

$$(Q^e v_m^*)' + \Omega^2 R^s u_m^* + \Omega^2 \lambda_m^* W^s u_m^* = 0, \quad (3.6b)$$

where a prime denotes a derivative with respect to the argument, $v = u'$. u_n and u_m^* satisfy the same boundary conditions. Since both equations are real and self-adjoint, the eigenfunctions and eigenvalues are real in both cases. Since Q^e, R^s, W^s are slowly varying large scale heterogeneities, the first $N = 2^j$ eigenfunctions of Eq. (3.6b) comprise macro-scales only. We shall restrict our discussion to these first N eigenfunctions. Note also that for these first N modes the smoothing rule in Eq. (3.5) is valid, because it results from relations between operator norms. We perform now an inner product of Eqs. (3.6a) and (3.6b) with u_m^* and u_n , respectively, and subtract the second from the first. The result is

$$\langle u_m^*, (Qv_n)' \rangle - \langle u_n, (Q^e v_m^*)' \rangle + \Omega^2 \lambda_n \langle u_m^*, W u_n \rangle - \Omega^2 \lambda_m^* \langle u_n, W^s u_m^* \rangle + \Omega^2 \langle u_m^*, R^d u_n \rangle = 0. \quad (3.7)$$

Perform now the following steps. Apply integration by parts to the two leftmost terms. Use the fact that $\langle u_n, W^s u_m^* \rangle = \langle u_n^s, W^s u_m^* \rangle$ (since W^s and u_m^* ($m \leq N = 2^j$) are macro-scale quantities). Multiply the last quantity by λ_n and add and subtract it from the last equation. The result is

$$u_m^* Q v_n|_a^b - u_n Q^e v_m^*|_a^b + \langle v_n, Q^e v_m^* \rangle - \langle v_m^*, Q v_n \rangle + \Omega^2 (\lambda_n - \lambda_n^*) \langle u_n^s, W^s u_m^* \rangle + \Omega^2 \lambda_n \langle u_m^*, W u_n - W^s u_n^s \rangle + \Omega^2 \langle u_m^*, R^d u_n \rangle = 0. \quad (3.8)$$

We have $u_m^* = \mathbf{P}_j u_m^*$, and \mathbf{P} is self-adjoint. Thus

$$\langle u_m^*, W u_n \rangle - \langle u_m^*, W^s u_n^s \rangle = \langle u_m^*, W^d u_n^d \rangle, \quad (3.9a)$$

$$\langle u_m^*, R^d u_n \rangle = \langle u_m^*, R^d u_n^d \rangle, \quad (3.9b)$$

$$\langle v_m^*, Q v_n \rangle = \langle \mathbf{P}_j v_m^*, Q v_n \rangle = \langle v_m^*, Q^e v_n^s \rangle \quad (\text{by Eq. (3.5) as the microscale } \ell \rightarrow 0). \quad (3.9c)$$

Substituting everything back into Eq. (3.8), we find

$$\langle u_n^s, W^s u_m^* \rangle (\lambda_n - \lambda_n^*) = [u_n Q^e v_m^* - u_m^* Q v_n]_a^b - \langle v_n^d, Q^e v_m^* \rangle - \Omega^2 \langle u_m^*, (R^d + \lambda_n W^d) u_n^d \rangle. \quad (3.10)$$

Let ℓ be the micro-scale — the length-scale on which u_n^d, v_n^d vary, and L_m^* be the length-scale on which u_m^* varies. Since the effective formulation consists of large scale coefficients only, it follows that L_m^* is determined only by the mode order, and is approximately $1/m$. It is clear that the two rightmost terms in Eq. (3.10) vanish as the parameter ℓ goes to zero (see Eqs. (2.13) and (2.17)). This fact is used next to establish a spectral equivalence between the effective and complete BVPs.

Homogeneous Neumann or Dirichlet boundary conditions. In this case the first term in the r.h.s. of Eq. (3.10) vanishes. Then

$$(\lambda_n - \lambda_n^*) \langle u_n^s, W^s u_m^* \rangle = -\langle v_n^d, Q^e v_m^* \rangle - \Omega^2 \langle u_m^*, (R^d + \lambda_n W^d) u_n^d \rangle \rightarrow 0 \quad \text{as } \frac{\ell}{L_n^*} \rightarrow 0 \quad \forall n \neq m. \quad (3.11)$$

Then by Eq. (3.11) and Theorem 3.1, we get

$$u_n^s \rightarrow u_n^* \quad \text{as } \frac{\ell}{L_n^*} \rightarrow 0, \quad (3.12a)$$

and with this last result, Eq. (3.11) gives (with $m = n$)

$$\lambda_n \rightarrow \lambda_n^* \quad \text{as } \frac{\ell}{L_n^*} \rightarrow 0. \quad (3.12b)$$

This is the “spectral equivalence” discussed in issue (3) in Section 1. From the rightmost term in Eq. (3.11) it is seen that for constant ℓ, L , the spectral equivalence becomes less accurate as the frequency Ω increases or as λ_n increases.

Impedance boundary conditions. Here, the first term on the r.h.s. of Eq. (3.10) does not vanish. The consequences are that in general $u_n^s \neq u_n^*$ and $\lambda_n \neq \lambda_n^*$.

Natural impedance boundary conditions. Let us consider the following boundary conditions:

$$Q(x)v(x) + \alpha_{1,2}u(x) = 0 \quad \text{at } x = a, b \quad (3.13a)$$

for the complete formulation, and

$$Q^e(x)v^*(x) + \alpha_{1,2}u^*(x) = 0 \quad \text{at } x = a, b \quad (3.13b)$$

for the effective formulation. With these BC $Qv_n = -\alpha_{1,2}u_n$ and $Q^e v_m^* = -\alpha_{1,2}u_m^*$ at the boundaries. Under these conditions the first term on the r.h.s. of Eq. (3.10) vanishes and Eqs. (3.12a) and (3.12b) hold again. This result is

of particular importance, as the impedance BC given in Eq. (3.13a) is used in many physical problems (see, for example, Section 3.2 in [17]). The fact that the identities in Eqs. (3.12a) and (3.12b) hold when the impedance BC of Eq. (3.13b) is applied to the effective formulation means that the effective measure of Q is also the relevant one for establishing the effective modes in the impedance case. These results are consistent with Table 1. Also here, when we increase Ω or λ_n the spectral equivalence “deteriorates”.

3.1.2. The effective Wronskian — a generalized spectral equivalence

An alternative approach to the spectral equivalence is to study the relation between the Wronskian of the complete problem, \mathcal{W} , and that of the effective one (*effective Wronskian*) \mathcal{W}^e . We have $\mathcal{W}[u_\ell, u_r] = u_\ell v_r - v_\ell u_r$ ($v = u'$), where u_ℓ, u_r are solutions of the source-free problem satisfying the left and right boundary conditions. It is well known that (with $M(x) = R(x) + \lambda W(x)$):

$$Q(x)\mathcal{W}[u_\ell, u_r] = \text{const.} = f(\Omega, \lambda), \quad (3.14)$$

that is, f is a function of the frequency parameter Ω and the spectral parameter λ , but *not* of x . Operating with \mathbf{P}_j (see Eq. (2.1a)) on both sides and using Eq. (3.5), we find that

$$Q^e(u_\ell^s v_r^s - v_\ell^s u_r^s) = f(\Omega, \lambda) \quad \text{as } \frac{\ell}{L} \rightarrow 0. \quad (3.15)$$

However, $u_\ell^s v_r^s - v_\ell^s u_r^s$ is nothing but the Wronskian associated with the macro-scale formulation and its solutions. Thus, Eqs. (3.14) and (3.15) yield the *Wronskian equivalence*

$$Q^e \mathcal{W}^e = Q \mathcal{W} = f(\Omega, \lambda) \quad \text{as } \frac{\ell}{L} \rightarrow 0. \quad (3.16)$$

That is, as $\ell/L \rightarrow 0$, the dependence of \mathcal{W}^e on Ω, λ approaches that of \mathcal{W} . It is well known that for a fixed Ω , the roots of \mathcal{W} and \mathcal{W}^e in the complex λ plane are λ_n and λ_n^* . Thus, this result re-establishes the spectral equivalence (3.12b). More important, the relation between \mathcal{W} and \mathcal{W}^e yields a spectral equivalence result in the complex Ω plane too. Let Ω_n, λ and Ω_n^*, λ be the roots of \mathcal{W} and \mathcal{W}^e in the complex Ω plane, for a fixed λ . Then, the last results yield

$$\Omega_n^*(\lambda) \rightarrow \Omega_n(\lambda) \quad \text{as } \frac{\ell}{L} \rightarrow 0. \quad (3.17)$$

These results are important for establishing effective modal representations, as well as for *effective resonance frequency* analysis (effective SEM). The temporal frequency equivalence was demonstrated numerically in [16].

3.1.3. Numerical example

Let us check the spectral equivalence via a simple numerical example. Consider the heterogeneity functions

$$Q(x) = W(x) = 1 + a \cos(\kappa \pi x), \quad \kappa \gg 1, \quad (3.18)$$

which have a typical length-scale of $\ell = 2/\kappa$. Thus, for $\Omega = 1$ these heterogeneity functions vary on the micro-scale. The effective properties are given, approximately, by

$$Q^e = \sqrt{1 - a^2}, \quad W^e = 1. \quad (3.19)$$

We have computed the eigenvalues and eigenfunctions of the complete problem (λ_n, u_n) , and those of the effective problem (λ_n^*, u_n^*) , for Neumann, Dirichlet, and natural impedance BC. The spectral equivalence is demonstrated in Fig. 4 for the eigenvalues. It is seen that the relative difference between the effective and complete spectra is kept below 1% for $n \leq \frac{1}{8}\kappa$ ($\approx 4/\ell$). Similar results were obtained for the modes (see more examples in Section 4).

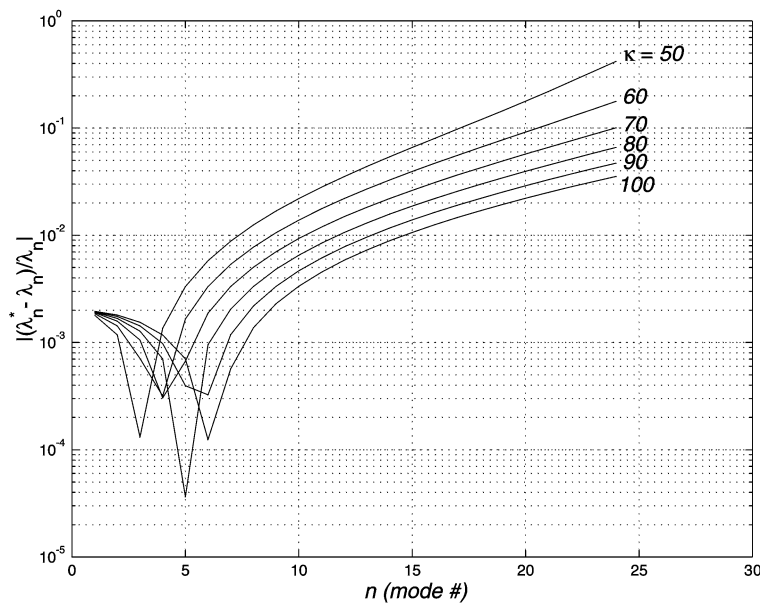
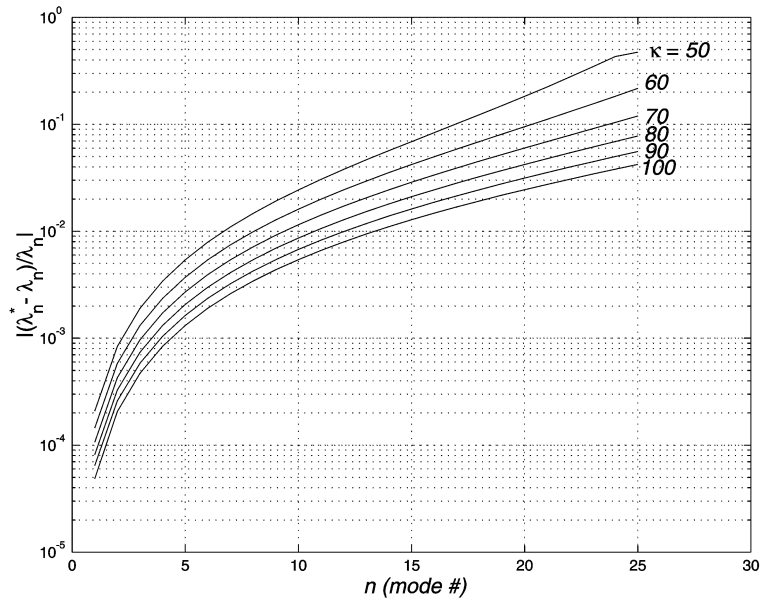


Fig. 4. The spectral equivalence: a comparison of the relative difference between the eigenvalues of Eq. (3.1) — the complete problem, and those of Eq. (3.4a) — the effective, or homogenized, problem. The heterogeneity functions are given in Eqs. (3.18) and (3.19) with $a = 0.5$: (a) Dirichlet BC, (b) Neumann BC, (c) natural impedance BC.

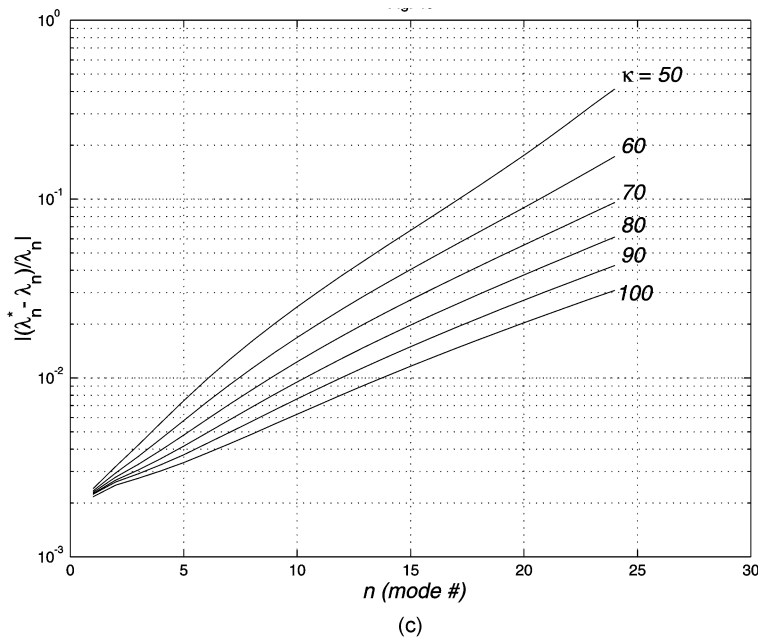


Fig. 4 (Continued).

3.2. Multi-resolution homogenization of propagation in complex laminates

Electromagnetic wave propagation in an isotropic plane stratified 2D medium is governed by

$$\nabla \cdot (\mathcal{Q}\nabla u) + k_0^2 g u = s(x, y), \quad \mathcal{Q} = p^{-1}\mathbf{I}, \quad 0 \leq x \leq a, \tag{3.20}$$

where $u(x, y)$ is the field, k_0 is a reference wavenumber, $s(x, y)$ is a source term, $p(x)$ and $g(x)$ represent the medium heterogeneity, and \mathbf{I} is the identity matrix. For TE or TM wave, u is the z -directed electric or magnetic field and $p(x) \equiv \mu(x)$, $g(x) \equiv \epsilon(x)$ or $p(x) \equiv \epsilon(x)$, $g(x) \equiv \mu(x)$, respectively. Eq. (3.20) is accompanied by boundary conditions at $x = 0, a$, and by an outgoing wave radiation condition at $|y| \rightarrow \infty$. It is assumed throughout that p and g vary rapidly in the x (vertical) direction and slowly in the y (horizontal) direction, when compared to the reference wavelength $\lambda = 2\pi/k_0$. The geometry is shown in Fig. 5. Our goal is to establish an homogenized representation of the problem, which incorporates effective measures of the complexity in the x -direction.

Eq. (3.20) can be reduced to a 1D Sturm–Liouville problem by a Fourier transform along the y coordinate. We define the transform pair

$$\tilde{u}(x, \eta) = \int_{-\infty}^{\infty} u(x, y) e^{-ik_0\eta y} dy, \quad u(x, y) = \frac{k_0}{2\pi} \int_{-\infty}^{\infty} \tilde{u}(x, \eta) e^{ik_0\eta y} d\eta. \tag{3.21}$$

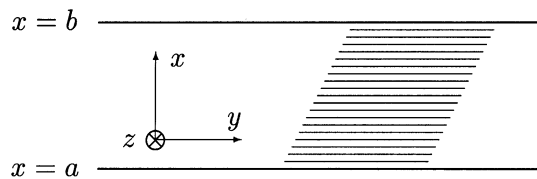


Fig. 5. The geometry of the complex laminate.

Upon applying it to the wave equation we get an ODE for \tilde{u} :

$$\left[\frac{d}{dx} Q(x) \frac{d}{dx} + k_0^2 M(x) \right] \tilde{u}(x, \eta) = \tilde{s}(x, \eta), \quad Q(x) = \frac{1}{p(x)}, \quad M(x) = g(x) - \frac{\eta^2}{p(x)}. \quad (3.22)$$

The large scale solution component, in the x -direction, is governed by

$$\left[\frac{d}{dx} Q^e \frac{d}{dx} + k_0^2 M^e \right] \tilde{u}^s(x, \eta) = \tilde{s}, \quad Q^e(x) = \frac{1}{p^s(x)}, \quad M^e(x) = g^s(x) - \eta^2 \left[\frac{1}{p(x)} \right]^s. \quad (3.23)$$

Applying the inverse Fourier transform, we obtain the effective wave equation

$$\nabla \cdot (\mathcal{Q}^e \nabla u^s) + k_0^2 g^e u^s = 0, \quad g^e(x) = g^s(x), \quad \mathcal{Q}^e(x) = \text{diag} \left\{ \frac{1}{p^s(x)}, \left[\frac{1}{p(x)} \right]^s \right\}. \quad (3.24)$$

This formulation is identical in form to Eq. (3.20) except that the heterogeneities \mathcal{Q} and g are replaced by their effective measures \mathcal{Q}^e and g^e obtained by smoothing in the x -direction. In general $1/p^s \neq (1/p)^s$. This introduces an effective anisotropy into the macro-scale formulation in Eq. (3.24). The anisotropy principal axes coincide with the stratification axes.

3.2.1. The spectral equivalence and modal representation of wave fields

We turn now to use the spectral equivalence results of Sections 3.1.1 and 3.1.2 to derive an effective modal expansion scheme in a waveguide. Let $\tilde{u}_n(x)$, η_n^2 and $\tilde{u}_n^*(x)$, $(\eta_n^2)^*$ be the eigenfunctions and eigenvalues associated with the complete and effective problems of Eqs. (3.22) and (3.23), respectively. The spectral equivalence demonstrated in Section 3.1.1 directly apply. Thus, we have

$$\tilde{u}_n^* \rightarrow \tilde{u}_n^s, \quad \eta_n^* \rightarrow \eta_n \quad \text{as} \quad \frac{\ell}{L_n^*} \rightarrow 0. \quad (3.25)$$

This equivalence is demonstrated in Section 4. The corresponding *propagation* modes are

$$u_n(x, y) = \tilde{u}_n(x) e^{ik_0 \eta_n y}, \quad (3.26a)$$

$$u_n^*(x, y) = \tilde{u}_n^*(x) e^{ik_0 \eta_n^* y}. \quad (3.26b)$$

Thus, in view of the spectral equivalence, the effective modes have the same x dependence as that of the macro-scale component of the complete ones, and the same propagation constants as those of the complete ones. Since $|\eta_n - \eta_n^*|$ is a *fraction of a percent* (see Section 3.1.3), it follows that for the lowest modes the homogenized formulations *keep track of the correct phase accumulation for hundreds of wavelengths*, at least in the asymptotic sense pointed in Eq. (3.25). The importance of this fact cannot be overemphasized.

Consider now an initial illumination field $u_0(x)$ at $y = 0$. Formal modal expansion of the field in the complete and homogenized formulations are given, respectively, by

$$u(x, y) = \sum_{n=1}^{\infty} \langle u_0, \tilde{u}_n \rangle \tilde{u}_n(x) e^{ik_0 \eta_n y} = \sum_{n=1}^{\infty} \langle u_0, \tilde{u}_n^s \rangle \tilde{u}_n(x) e^{ik_0 \eta_n y} \quad (\text{by (2.13) and (2.17) as } \ell \rightarrow 0), \quad (3.27a)$$

$$u^*(x, y) = \sum_{n=1}^N \langle u_0, \tilde{u}_n^* \rangle \tilde{u}_n^*(x) e^{ik_0 \eta_n^* y}, \quad (3.27b)$$

where the upper limit of the summation in the latter, N , is chosen as to include scales consistent with the pre-defined smoothing level j . Thus $N = 2^j$ (assuming a laminate width of unity). Under this condition, the spectral equivalence holds and one has

$$u^* = \mathbf{P}_j u = u^s. \quad (3.28)$$

3.2.2. The Green function

The one-dimensional Green function $\tilde{G}(x, \eta; x', y')$ of the complete problem (3.20)–(3.22) can be expressed by the modal summation [17]

$$\tilde{G}(x, \eta; x', y') = -\sum_n \frac{\tilde{u}_n(x)\tilde{u}_n(x')}{\eta^2 - \eta_n^2} e^{-i\eta y'}. \quad (3.29)$$

When the last expression and the inverse transform, Eq. (3.21), are used in conjunction with the Residue theorem, we get the modal representation of $G(x, y; x', y')$:

$$G(x, y; x', y') = \frac{ik_0}{2} \sum_n \frac{\tilde{u}_n(x)\tilde{u}_n(x')}{\eta_n} e^{ik_0\eta_n|y-y'|}. \quad (3.30)$$

Formally, the Green function of the effective problem is given by the same summation, with u_n, η_n replaced by the corresponding quantities of the homogenized formulation u_n^*, η_n^* . This, however, yields the response for a $\delta(x-x')$ source, which is inconsistent with the initial requirements from the homogenized formulation; the solutions associated with the latter should not contain, at least formally, any micro-scale component. Furthermore, summation of elements with increasingly large n must include building blocks for which the spectral equivalence breaks down.

The way to circumvent this inconsistency is to redefine the role of G , as to match the ideas behind macro-scale formulations. The effective Green function should be the response to a source excitation from which all and *only* large scale sources can be obtained. Thus, it is the response to the *smoothed* δ , containing only the spectral components in the interval $|\xi| \leq 2^j$. The corresponding Green function, termed now the *effective* Green function, is given by

$$G^e(x, y; x', y') = \frac{ik_0}{2} \sum_{n=1}^{N=2^j} \frac{\tilde{u}_n^*(x)\tilde{u}_n^*(x')}{\eta_n^*} e^{ik_0\eta_n^*|y-y'|}, \quad (3.31)$$

which is now consistent with the idea of large scale solutions. Furthermore, for this range of summation, the spectral equivalence holds, thus G^e can be expressed also as $\mathbf{P}_j \mathbf{P}'_j G(x, z; x', z')$, where \mathbf{P}_j and \mathbf{P}'_j act on the x and x' dependence, respectively. This establishes a “horizontal” connection between the complete and effective Green functions (see Fig. 2).

4. Numerical examples

Consider a propagation of a TM wave in a complex laminate with boundaries at $a = 0, b = 1$, with $\mu = 1$, and with the complex ϵ heterogeneity described in Fig. 1. The inner scale of this heterogeneity is $\ell = 0.02$. We choose $k_0 = 5\pi$ that corresponds to a wavelength $\lambda = 0.4$, 20 times larger than ℓ . For this range of parameters, an appropriate smoothing level is $j = 4$. Also, spectral equivalence should hold well for the first few modes. Fig. 6 shows $1/p^s$ and $(1/p)^s$ associated with $p(x)$. Fig. 7 shows η_m^2 (\times signs) and $(\eta_m^2)^*$ ($+$ signs) associated with $p(x)$ of Fig. 1 and with its effective measures (of Fig. 6), respectively. To appreciate the effects of the heterogeneity, we also show by circles η_m^2 in the absence of the heterogeneity ($p(x) = 1$). Fig. 8 shows the corresponding first three modes associated with the complete (solid) and with the effective (dash-dot) formulation. The latter are smoother, but convey the same large scale behavior. These results demonstrate the efficacy of large scale modal representations.

5. Conclusions

Multi-resolution theory and wavelets expansion were used to develop homogenized formulation for propagation in complex laminates. This formulation governs the propagation of the field macro-scale component. The connection

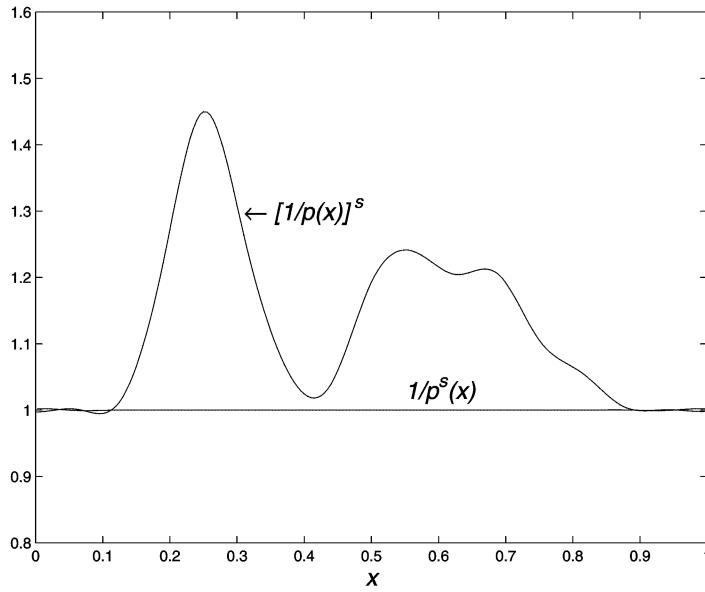


Fig. 6. The effective measures associated with the heterogeneity of Fig. 1.

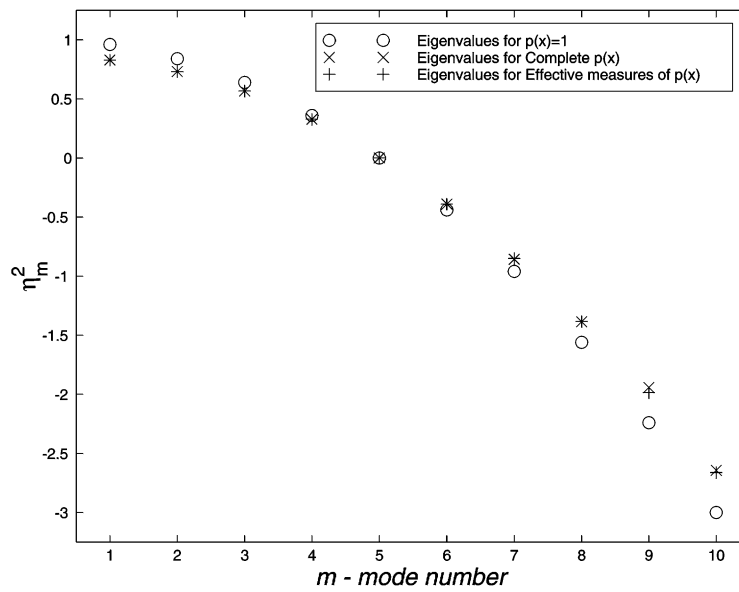


Fig. 7. The eigenvalues. Shown are η_m^2 (\times signs), $(\eta_m^2)^*$ ($+$ signs), and η_m^2 associated with the homogeneous problem $p = 1$ (\circ signs).

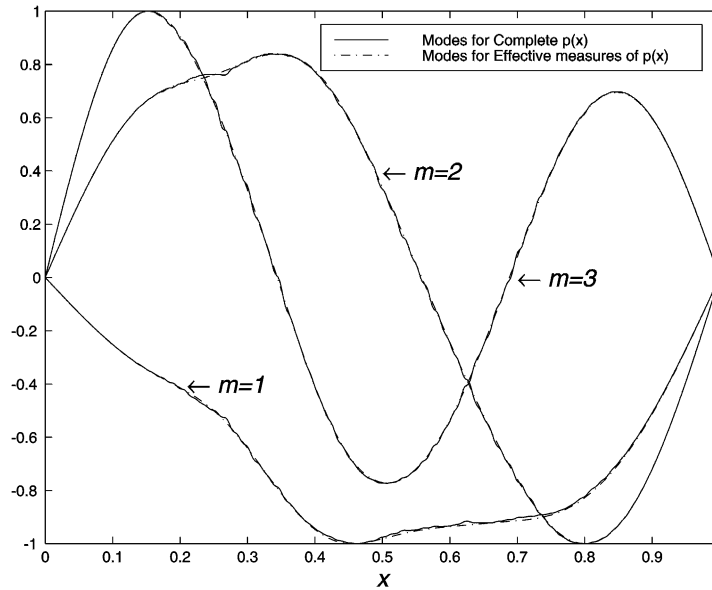


Fig. 8. The first three modes. Shown are \tilde{u}_n and \tilde{u}_n^* .

between the basic entities associated with the complete formulation (such as boundary conditions, modes, eigenvalues, resonances, modal expansions) and those of the homogenized one was investigated. A central issue here is the spectral equivalence (or more generally, the Wronskian equivalence) and its dependence on the micro-scale. It is shown that spectral equivalence holds for modes satisfying $L_m^* \gg \ell$, the former is the length-scale on which the m th effective mode varies, and the latter is the micro-scale. Self-consistent effective modal expansion scheme and effective Green function representation were suggested.

Acknowledgements

This research was supported in part by a grant from the Israel Science Foundation.

Appendix A. Derivation of integral equations

Case 1 is the simplest one. Define the background Green function $G(x; y)$ as that associated with the homogeneous medium $Q = M = 1$, with the same BC as for Eq. (3.1). The solution for G is straightforward and can be found in many textbooks. It is continuous at $x = y$ and varies on the macro-scale dimension for $x \neq y$. An integral equation formulation is obtained by moving $m(x)$ to the differential equation r.h.s., and expressing the solution $u(x)$ as a convolution of G with the extended source term $F(x) - \Omega^2 m(x)u(x)$. The result is given by the formulation in Eqs. (2.2a) and (2.2b) with $k(x, y) = G(x, y)$, $q = m$, and $u_0 = \int F(y)G(x, y) dy$. Recalling the regularity properties of G , this case corresponds to the one described in Section 2.2.1. The key point here is that u^s satisfies, to a good approximation, the same integral equation (i.e. the same kernel) as that of u , with M replaced by M^s . That means u^s satisfies also the corresponding complete differential equation with M replaced by M^s , and with the same boundary conditions.

In case 2, the procedure leading to an integral equation is somewhat more involved. First, we move the term $(qu)'$ to the r.h.s. of the differential equation governing u . Then, we use G of case 1 to express u as a convolution with the extended source term $F - (qu)'$. The result is an integro-differential equation for u ,

$$u(x) = u_0(x) + \int_a^b G(x, y)(q(y)u'(y))' dy. \quad (\text{A.1})$$

Taking a derivative with respect to x , defining $v = u'$, and performing integration by parts, we obtain an integral equation for v in the form discussed in Section 2.2.2 with $k(x, y) = \partial_{xy}^2 G(x, y) = \Gamma(x, y) - \delta(x - y)$, where Γ is continuous at $x = y$ (see [8] for details). The results of Section 2.2.2 directly apply

$$Q^e(x) = [(Q^{-1})^s]^{-1}. \quad (\text{A.2})$$

However, due to the integration by parts, the forcing and Γ generally depend now on the *numbers* $q(a)$, $q(b)$. Thus, while the structure of the equation is preserved, the effective formulation cannot be obtained from the complete one by a mere replacement $q \rightarrow q^e$. The dependencies on $q(a)$, $q(b)$ cancel only for the three cases of boundary conditions summarized in the left column of Table 1, and these are the only cases that one can define boundary conditions to be applied on u^s . The corresponding effective BC are summarized in the table. Finally, we note that the smoothing rule of Eq. (2.18) holds, but for $v = u'$, the quantity governed by the integral equation.

References

- [1] V.V. Jikov, S.M. Kozlov, O.A. Oleinik, *Homogenization of Differential Operators and Integral Functionals*, Springer, Berlin, 1994.
- [2] B.Z. Steinberg, J.J. McCoy, Towards local effective parameter theories using multiresolution decomposition, *J. Acoust. Soc. Am.* 96 (1994) 1130–1143.
- [3] B.Z. Steinberg, J.J. McCoy, Effective measures for non-stationary micro-scale stiffness variation using multiresolution decomposition, *J. Acoust. Soc. Am.* 98 (6) (1995) 3516–3526.
- [4] B.Z. Steinberg, J.J. McCoy, A class of one-dimensional stiffness microstructures resulting in identical macro-scale response, *Wave Motion* 23 (1996) 237–258.
- [5] B.Z. Steinberg, J.J. McCoy, A multiresolution study of effective properties of complex electromagnetic systems, *IEEE Trans. Antennas Propag.* 26 (1998) 971–981.
- [6] B.Z. Steinberg, J.J. McCoy, A study of the effective properties of mass and stiffness microstructures — a multiresolution approach, *Quart. J. Appl. Math.* 57 (1999) 401–432.
- [7] B.Z. Steinberg, J.J. McCoy, A multiresolution analysis of scattering by a pair of local regions of complex heterogeneity, *J. Acoust. Soc. Am.* 103 (3) (1998) 1273–1281.
- [8] B.Z. Steinberg, J.J. McCoy, M. Miroznik, A multiresolution approach to homogenization and effective modal analysis of complex boundary value problems, *SIAM J. Appl. Math.* 60 (3) 939–966 (published electronically, March 2000 at <http://www.siam.org/journals/siap/60-3/32369.html>).
- [9] B.Z. Steinberg, J.J. McCoy, A multiresolution homogenization of modal analysis with application to layered media, *Int. J. Math. Comput. Simul.* (special issue on direct and inverse scattering) 50 (1999) 393–417.
- [10] I. Daubechies, *Ten Lectures on Wavelets*, CBMS–NSF Series in Applied Mathematics, SIAM, Philadelphia, PA, 1992.
- [11] B.Z. Steinberg, J. Oz, A multiresolution approach for the effective properties of complex propagation ducts and effective modes/rays theories, in: *Proceedings of the 1998 URSI International Symposium on Electromagnetic Theory*, Thessaloniki, Greece, May 25–28, 1998.
- [12] B.Z. Steinberg, E. Heyman, Effective vertical modes and horizontal rays for wave propagation in complex inhomogeneous ducts, in: *Proceedings of the 1998 URSI International Symposium on Electromagnetic Theory*, Thessaloniki, Greece, May 25–28, 1998.
- [13] M.E. Brewster, G. Beylkin, A multiresolution strategy for numerical homogenization, *Appl. Comp. Har. Anal.* 2 (1995) 327–349.
- [14] A.C. Gilbert, A comparison of multiresolution and classical one-dimensional homogenization schemes, *Appl. Comp. Har. Anal.* 5 (1998) 1–35.
- [15] G. Beylkin, N. Coult, A multiresolution strategy for reduction of elliptic PDEs and eigenvalue problems, *Appl. Comp. Har. Anal.* 5 (1998) 129–155.
- [16] B.Z. Steinberg, Effective modal and spectral representation of propagators in complex ducts — a multiresolution and homogenization approach, in: *Proceedings of the International Conference on Electromagnetics in Advanced Applications (ICEAA'99)*, Torino, Italy, September 13–17, 1999, pp. 345–347.
- [17] L.B. Felsen, N. Marcuvitz, *Radiation and Scattering of Waves*, Prentice-Hall, Englewood Cliffs, NJ, 1973.